Supplementary Information

A high-entropy iron-based perovskite rich in oxygen vacancies for enhanced oxygen reduction kinetics in intermediate-temperature SOFCs

Xiangsheng Yang[a], Qianqian Chai[a], Yang Wu [a,*], Jianli Wang[a, b], Yaoqiang Chen[a, b], and Haidi Xu [a,*]

a. Institute of New Energy and Low-Carbon Technology, Sichuan University, Chengdu, 610065, China

b. School of Chemistry, Sichuan University, Chengdu, 610065, China

*Corresponding author. Email: xuhaidi@scu.edu.cn (Haidi Xu); yangwu@scu.edu.cn and wuyang_scu@163.com (Yang Wu)

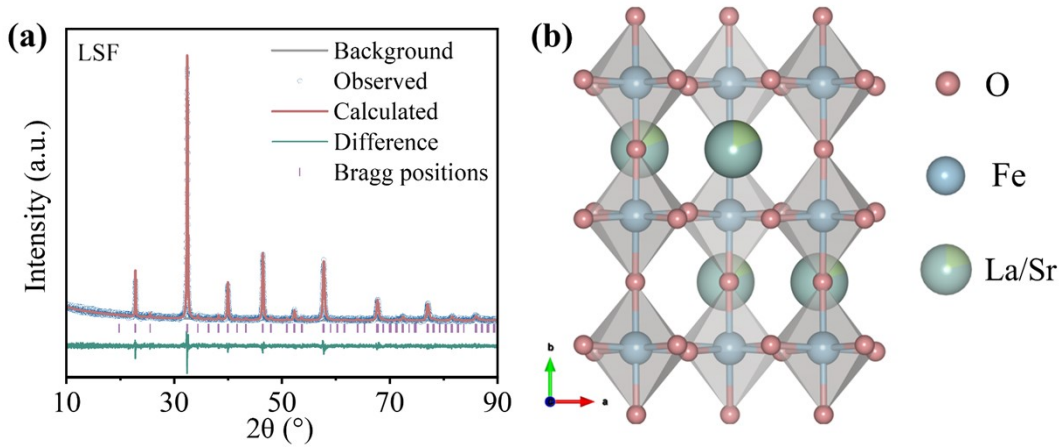

Figure S1. The XRD refinement results (a) and crystal structure model of the LSF (b).

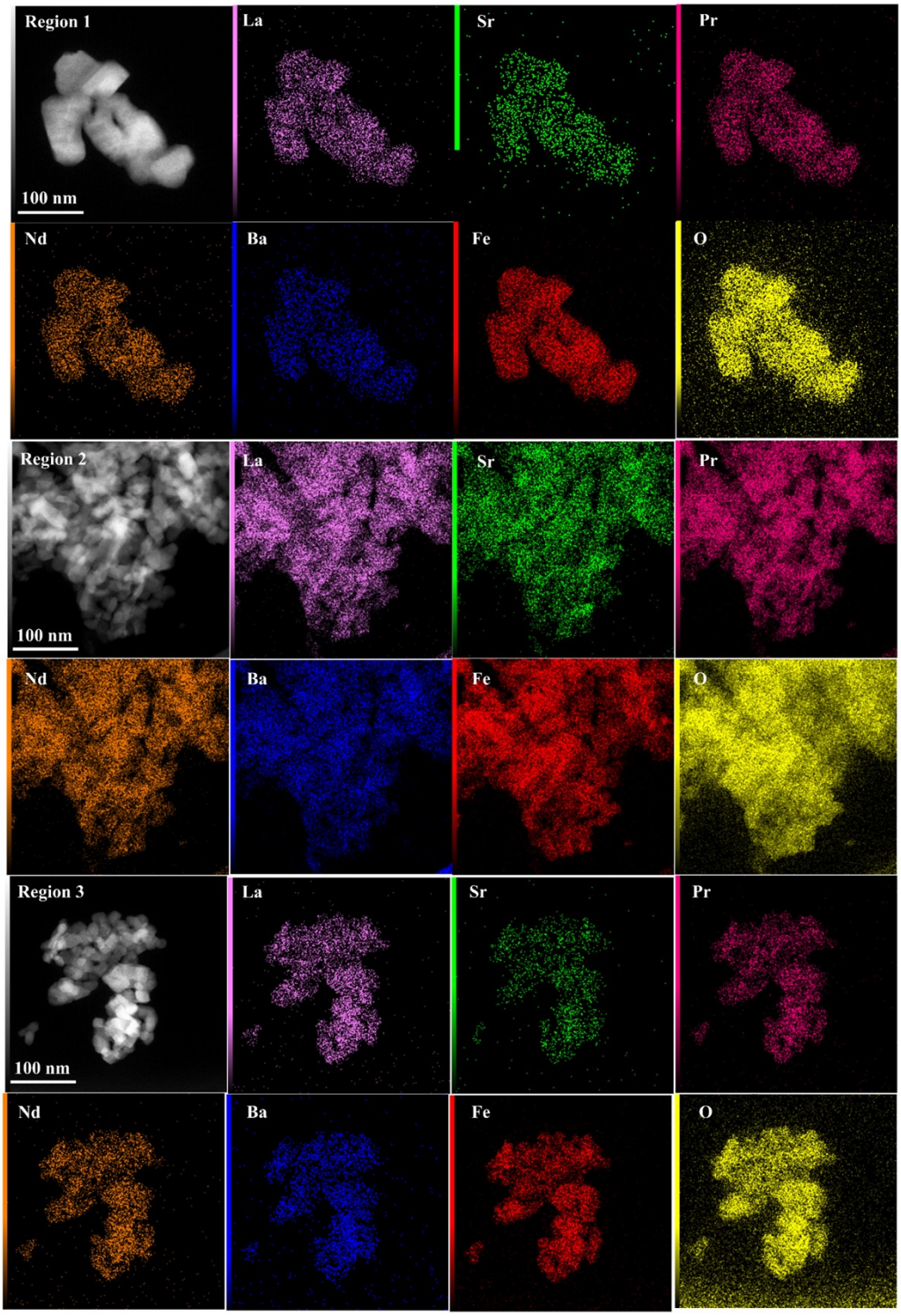

Figure S2. HAADF-STEM and EDX elemental mappings acquired from three representative regions of the HEP sample.

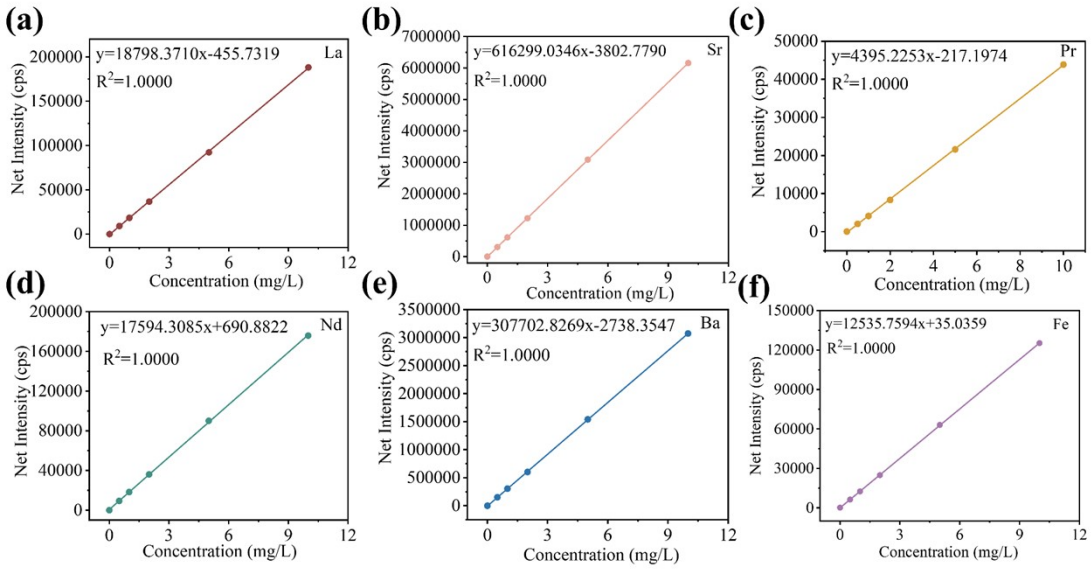

Figure S3. The ICP calibration curves for six target elements: La (a), Sr (b), Pr (c), Nd (d), Ba (e), and Fe (f).

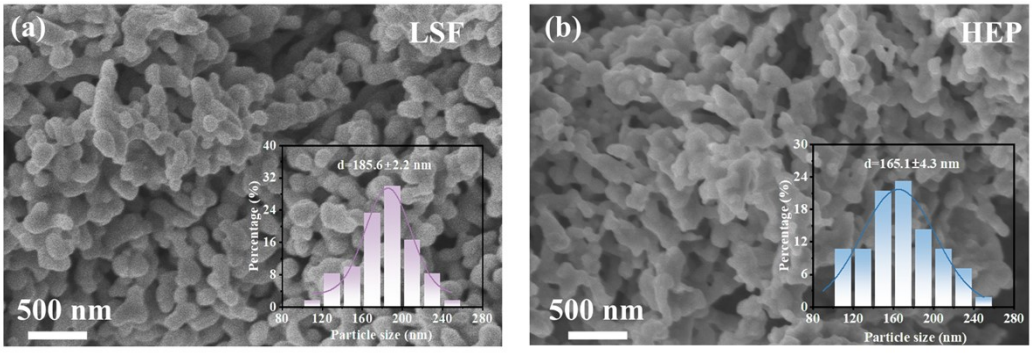

Figure S4. The SEM images of the LSF (a) and HEP (b), with insets showing particle size distributions.

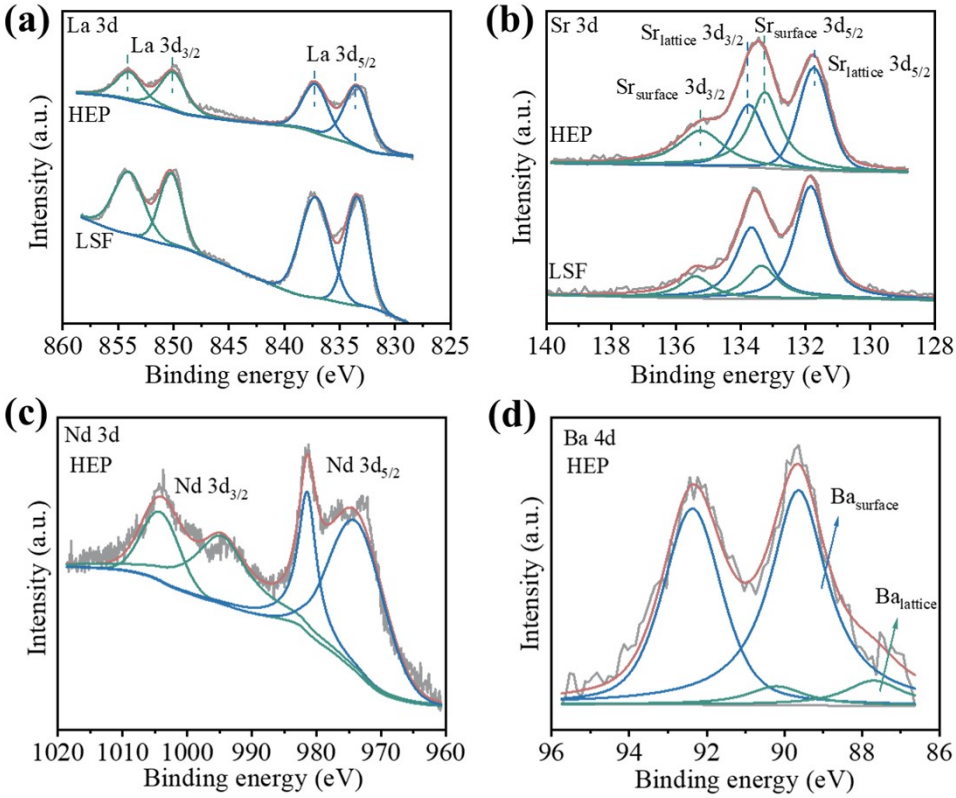

Figure S5. XPS La 3d spectra (a) and Sr 3d spectra (b) for the HEP and LSF. XPS Nd 3d spectra (c) and Ba 4d spectra (d) for the HEP.

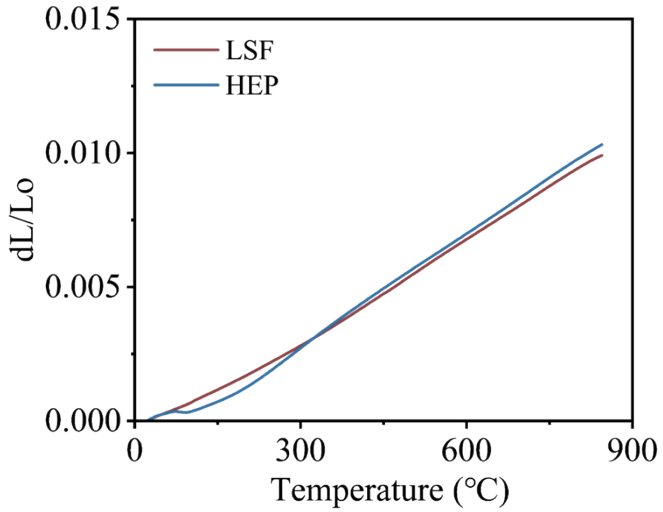

Figure S6. Thermal expansion properties for the HEP and LSF.

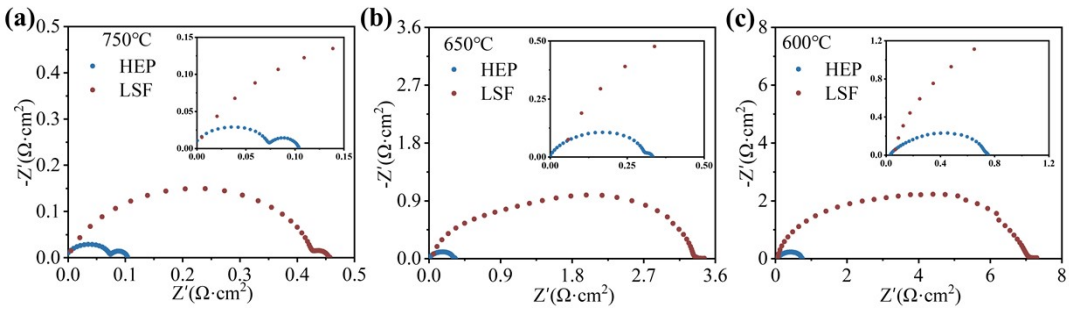

Figure S7. EIS of the symmetrical cells at 750 ℃ (a), 650℃ (b) and 600℃ (c).

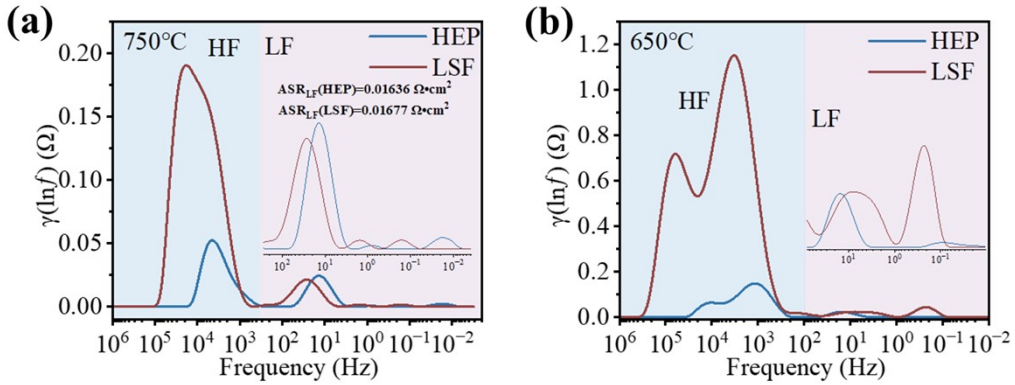

Figure S8. DRT analysis of the symmetric cells at 750 ℃ (a) and 650 ℃ (b).

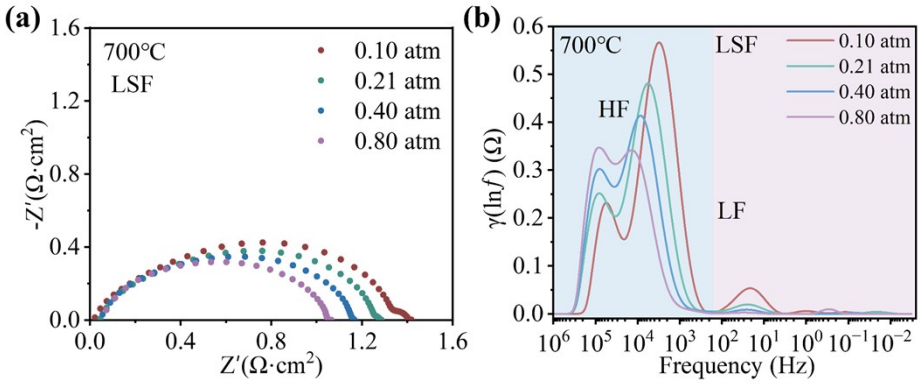

Figure S9. (a) EIS curves of the symmetric cells with the LSF electrode at 700 ℃ as a function of pO_2. (b) DRT analysis of the LSF as a function of oxygen partial pressure at 700℃.

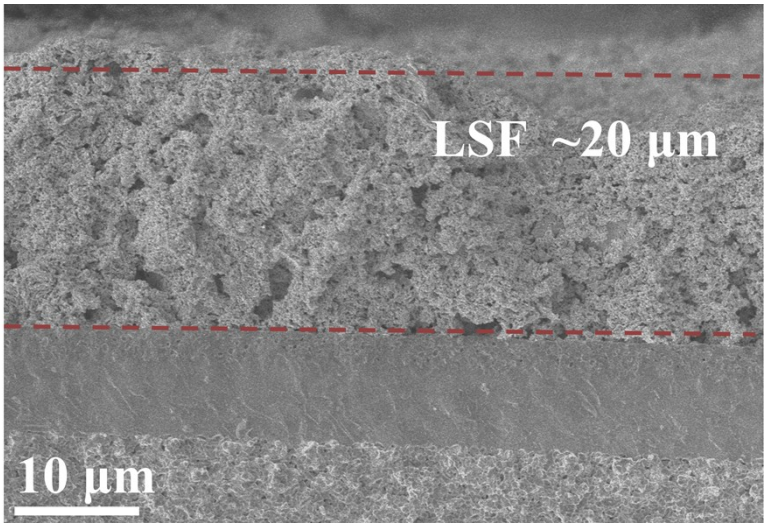

Figure S10. The Cross-sectional SEM micrograph of anode-supported single cell with the LSF cathode.

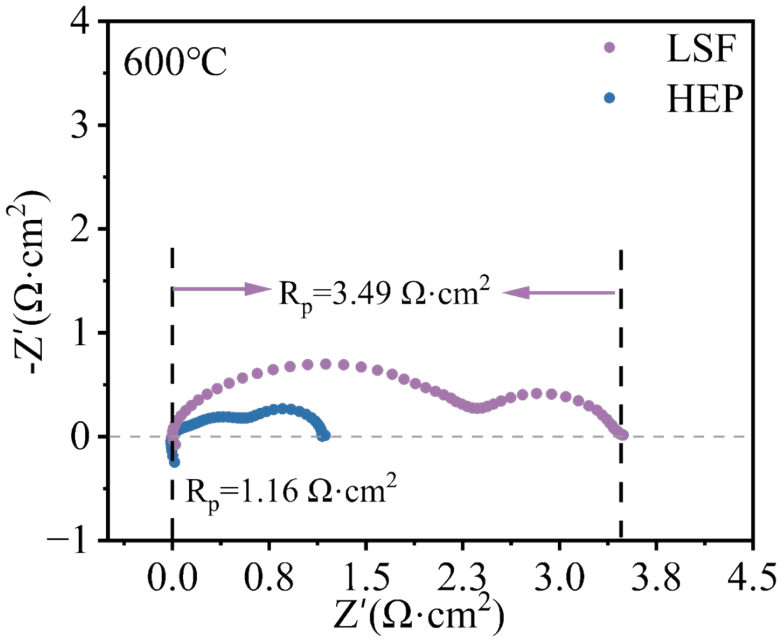

Figure S11. The EIS curves of anode-supported single cells at 600 °C.

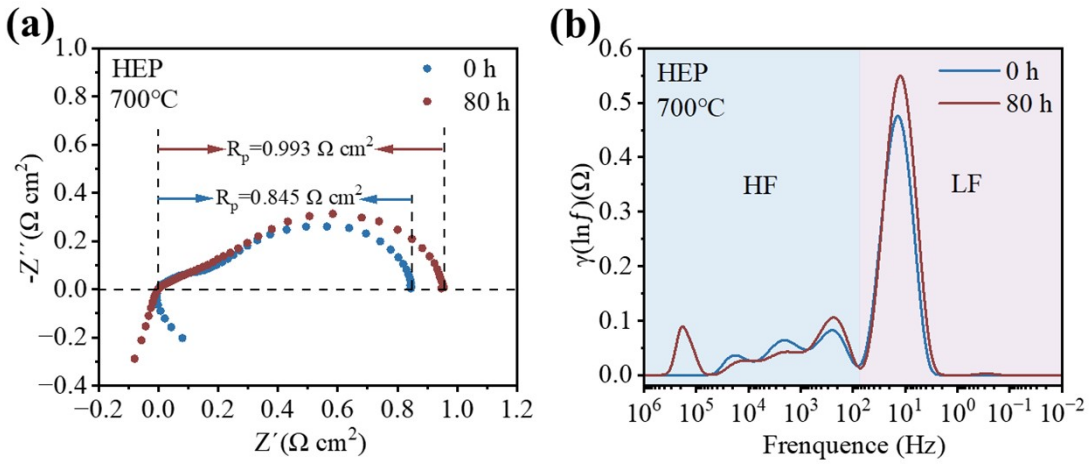

Figure S12. EIS curves (a) and the corresponding DRT analysis (b) of the anode-supported single cell at 700 °C at the initial state and after 80 h stability test.

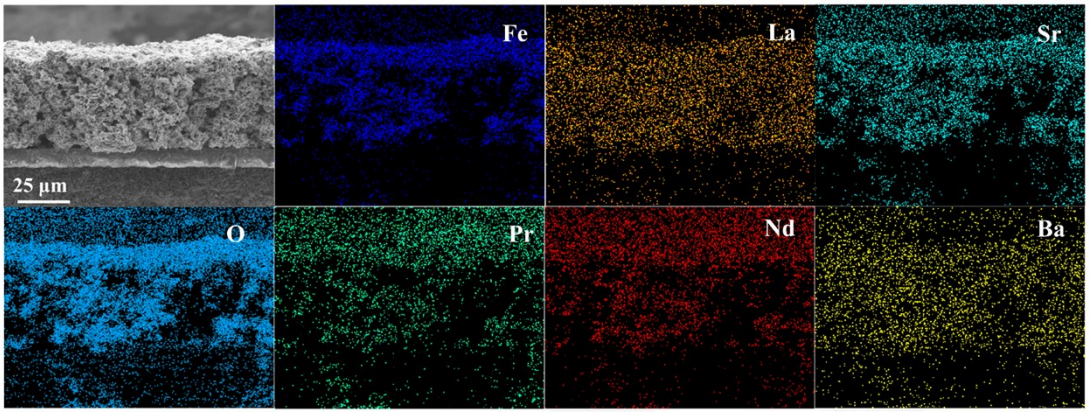

Figure S13. Cross-sectional SEM and EDX images of a single cell with the HEP as the cathode after an 80-hour stability test.

Table S1. Real and theoretical densities of the LSF and HEP determined by He-gas displacement method and X-ray Rietveld refinement, respectively.

Sample	Real density (g/cm^3)	Standard deviation (g/cm^3)	Theoretical density (g/cm^3)
LSF for CTE	6.5347	0.0015	6.423
LSF for σ	6.6017	0.0147	6.423
HEP for CTE	6.5190	0.0121	6.517
HEP for σ	6.5964	0.0056	6.517

The theoretical density is calculated using an ideal perfect crystal model free of crystal defects and impurities with strict stoichiometry, whereas the true density characterizes the real atomic packing compactness of the material. The higher measured true density compared with the theoretical density obtained from XRD Rietveld refinement is mainly because the refinement model does not fully account for internal crystal defects (e.g., oxygen vacancies), the actual stoichiometry of the sample deviates from the nominal value, and surface-adsorbed impurities introduce certain measurement errors.

Table S2. Refinement parameters of the LSF and HEP derived from XRD patterns.

Sample	LSF	HEP
Space group	Pnma	Pnma
Cell Volume ($Å^3$)	240.457	237.953
Lattice parameters		
a (Å)	5.54922	5.5206
b (Å)	7.83156	7.80463
c (Å)	5.53297	5.5227
R_p	7.35%	7.04%
R_{wp}	9.18%	8.98%
GOF	4.53	4.56

Table S3. Structural parameters of the HEP from XRD Rietveld refinement

Atom	Multiplicity	x	y	z	Occupancy	U_{iso} (Å^2)
O1	4	0.4996	0.25	0.5404	1	0.0303
O2	8	0.2983	0.012	0.1976	1	0.0167
Fe	4	0	0	0	1	0.0185
La	4	0.4779	0.25	0.0145	0.29	0.0189
Sr	4	0.4779	0.25	0.0145	0.2	0.0189
Pr	4	0.4779	0.25	0.0145	0.13	0.0189
Nd	4	0.4779	0.25	0.0145	0.15	0.0189
Ba	4	0.4779	0.25	0.0145	0.15	0.0189

Table S4. Structural parameters of the LSF from XRD Rietveld refinement

Atom	Multiplicity	x	y	z	Occupancy	U_{iso} (Å^2)
O1	4	0.4975	0.25	0.5696	1	0.0401
O2	8	0.2211	0.0124	0.2942	1	0.0107
Fe	4	0	0	0	1	0.0152
Sr	4	0.4794	0.25	0.0118	0.2	0.0123
La	4	0.4794	0.25	0.0118	0.8	0.0123

Table S5. Elemental atomic ratios obtained by TEM-EDX quantitative analysis.

Element	atomic ratio (%)			
	Region 1	Region 2	Region 3	average value
La	18.40	16.91	18.94	18.08
Sr	10.52	11.45	10.93	10.97
Pr	7.80	7.70	8.63	8.04
Nd	8.78	7.92	8.81	8.50
Ba	1.94	2.56	1.86	2.12
Fe	52.55	53.46	50.83	52.28

Normalized to the Fe content, the stoichiometric formula of the HEP is: $La_{0.35}Sr_{0.21}Pr_{0.15}Nd_{0.16}Ba_{0.04}FeO_{3-\delta}$.

Table S6. The atomic ratio of each element in the as-synthesized HEP, measured by ICP-OES.

Element	La	Sr	Pr	Nd	Ba	Fe
atomic ratio (%)	15.28	10.37	6.93	7.83	7.70	51.89

Normalized to the Fe content, the stoichiometric formula of the high-entropy perovskite is: $La_{0.29}Sr_{0.20}Pr_{0.13}Nd_{0.15}Ba_{0.15}FeO_{3-\delta}$.

Table S7. Quantitative analysis results based on XPS spectra.

Sample	Pr^{3+}/Pr^{4+} ratio	$Fe^{2+}/Fe^{3+}/Fe^{4+}$ ratio	$O_{lattice}/O_{ads}$ ratio
LSF	-	0.23/0.55/0.22	0.45/0.55
HEP	0.62/0.38	0.14/0.61/0.25	0.37/0.63

Table S8. The fitting results of Mössbauer spectroscopy.

Sample	Peak	IS (mm/s)	QS (mm/s)	H(T)	Γ (mm/s)	Assignment	Area (%)
HEP	Sextet 1	0.29	-0.30	27.57	1.88	LS Fe^{3+}	12.80
	Sextet 2	0.56	0.06	41.70	1.28	HS Fe^{3+}	32.70
	Sextet 3	-0.13	0.48	23.08	0.53	HS Fe^{4+}	6.70
	Sextet 4	0.47	0.01	50.11	0.71	HS Fe^{3+}	25.60
	Sextet 5	0.95	0.05	26.24	1.88	HS Fe^{2+}	2.90
	Sextet 6	0.42	-0.05	46.00	0.62	HS Fe^{3+}	9.30
	Doublet 1	0.38	1.56	-	0.83	HS Fe^{3+}	10.20
LSF	Sextet 1	1.23	-0.34	29.77	1.69	HS Fe^{2+}	6.50
	Sextet 2	0.50	-0.04	41.61	1.36	HS Fe^{3+}	36.60
	Sextet 3	-0.38	0.39	26.16	0.82	HS Fe^{4+}	4.50
	Sextet 4	0.48	-0.10	50.07	0.89	HS Fe^{3+}	29.60
	Sextet 5	0.25	-0.09	28.00	0.59	LS Fe^{3+}	4.30
	Sextet 6	0.53	-0.06	46.86	0.66	HS Fe^{3+}	14.50
	Doublet 1	0.39	2.05	-	0.40	HS Fe^{3+}	4.00

Table S9. Iodometric titration results of the LSF.

material mass (g)	the consumed volume of $Na_2S_2O_3$ (ml)	average oxidation state of Fe	δ
0.0916	3.96	+2.9981	0.1009
0.0907	3.93	+3.0005	0.0998
0.0931	4.10	+3.0174	0.0913

Based on the above results, the average oxidation state of Fe is calculated to be +3.0053, and the corresponding average oxygen non-stoichiometry δ is 0.0973.

Table S10. Iodometric titration results of the HEP.

material mass (g)	the consumed volume of $Na_2S_2O_3$ (ml)	average oxidation state of Pr	δ
0.0798	3.98	+3.3860	0.2509
0.0792	3.88	+3.4716	0.2453
0.0800	3.91	+3.2114	0.2623

The average Fe oxidation state of +3.04 is derived from Mössbauer spectroscopic results.

Based on the above results, the average oxidation state of Pr is calculated to be +3.3563, and the corresponding average oxygen non-stoichiometry δ is 0.2528.